Vietnam Journal of Science and Technology ***56*** *(1A) (2018) 127-134*

TAILORING THE STRUCTURE AND MORPHOLOGY OF WO_3 NANOSTRUCTURES BY HYDROTHERMAL METHOD

Luu Thi Lan Anh, Pham Tuan Phong, Han Viet Phuong, Duong Vu Truong, Le Xuan Vuong, Pham Trung Son, Do Duc Tho, Dang Duc Vuong, Nguyen Huu Lam, Nguyen Cong Tu*

School of Engineering Physics, Hanoi University of Science and Technology, No 1, Dai Co Viet street, Ha Noi

*Email: *tu.nguyencong@hust.edu.vn*

Received: 15 August 2017; Accepted for publication: 30 March 2018

ABSTRACT

Tungsten oxide nanostructures were synthesized by hydrothermal and acid precipitation (hydrothermal at room temperature) methods without using any supporting agent or structure-directing reactant. The morphology and crystalline structure of nanostructures strongly depended on pH of the precursor solution and synthesis method. With pH = -1.0, using acid precipitation method, orthorhombic nanoplate was observed. Using hydrothermal method, with the pH = -1.0, we obtained directly stable monoclinic nanoparticle WO_3. With pH = 1.1, the mixing of nanoparticle and nanorod with the hexagonal frame was acquired. When pH reaches to 1.7, only bundle of hexagonal nanorods was observed. To characterize the morphology and structure of tungsten nanostructures, we used Field Emission Scanning Electron Microscopy, X-ray diffraction, and micro Raman spectroscopy. The micro Raman spectroscopy was used to support the X-ray diffraction analysis. These results imply that adjusting pH is an efficient and promising method to manipulate both morphology and crystal structure of WO_3 nanostructure for selective applications.

Keywords: tungsten oxide, nanoparticle, nanoplate, nanorod, hydrothermal.

1. INTRODUCTION

Tungsten oxide (WO_3) is a metal oxide semiconductor with the band gap in the range of visible region [1]. Many groups have studied tungsten oxide for different applications such as photocatalyst [2], smart window [3] etc. In recent years, WO_3 appeared to be attractive materials for electrochemistry - electrode for lithium ion battery [4, 5], photocatalysis of water [1, 6, 7] and gas sensor [8-10]. For different applications, various nanostructures of WO_3 having different crystal structures or morphologies were designed. Poongodi *et al*. purposely synthesized WO_3 nanoplate for smart window [3], Marques *et al*. used WO_3 nanoparticles for the colorimetric detection of electrochemically active bacteria [11] etc.

The common methods to grow WO_3 nanostructure are acid precipitation [1], electrodeposition [3], solution combustion [5], and hydrothermal method [4, 7-10]. Because of the simplicity and flexibility, acid precipitation and hydrothermal methods are the most widely used methods. Using these methods, many efforts have been dedicated to finding the way to engineer or manipulate morphology [1, 11, 12], crystalline structure [11, 13, 14] and crystal facet [6, 15] of WO_3 nanostructures. In these works, both supporting agents, structure-directing reactant, and pH value are used as control parameters. Also using the hydrothermal and acid precipitation methods, in this study, our purpose is to synthesize and engineer WO_3 nanostructures without using any supporting agents. Especially, a simple method to directly grow stable monoclinic structure of WO_3 is also presented. We used only two precursors: sodium tungsten dehydrate ($Na_2WO_4.2H_2O$) and hydrochloric acid (HCl). To manipulate the morphology and crystal properties of WO_3 nanostructure, we tuned the pH value and temperature.

WO_3 has various crystal patterns such as monoclinic, triclinic, orthorhombic, tetragonal, cubic and hexagonal [2]. In addition, the natural appearance of phase $WO_{x(x<3)}$ having complex X-ray diffraction (XRD) patterns in WO_3 nanostructures makes crystal analyzing more difficult. To investigate the crystal structure of WO_3 nanostructures, the researcher used the combination of analysis techniques such as the combination of XRD and micro Raman spectroscopy [1, 12, 18]. Raman spectroscopy was also used to investigate the photocatalytic and electrochromic of WO_3 nanostructures [2, 3]. In this work, Micro Raman spectroscopy was used as a supplement for XRD analysis in investigating structure and morphology of WO_3 nanostructures.

2. MATERIALS AND METHODS

2.1. Sample preparation

In this paper, WO_3 nanostructures were synthesized by hydrothermal method or acid precipitation method (hydrothermal method at room temperature – RT) with two reactants: sodium tungsten dehydrate ($Na_2WO_4.2H_2O$), and hydrochloric acid (HCl) in analytical reagent level without any further purification. 8.25 g of $Na_2WO_4.2H_2O$ was dissolved in 25 mL of bi-distilled water under constant stirring at room temperature to get a transparent Na_2WO_4 solution. The buffer solution of HCl, then, was dropped gradually into the transparent solution to create H_2WO_4 as the following equation:

$$Na_2WO_4 + 2HCl \rightarrow H_2WO_4 + 2NaCl$$

The appearance of H_2WO_4 causes coloring of solution which changes from transparent to milk-like color and finally yellow. pH of solution was controlled with HCl buffer solution. After stirring for 4 hours, the obtained solution was put into Teflon-lined stainless-steel autoclave. In this work, we grew four WO_3 nanostructures: one sample synthesized by acid precipitation method with pH = -1.0 (labeled o-WO_3) and three samples synthesized by hydrothermal method in three different acidic environments (pH = -1.0, 1.1, 1.7 labeled m-WO_3, h-WO_3, hn-WO_3 respectively). The hydrothermal process was carried out at 180 ^oC or 120 ^oC for 48 hours. When hydrothermal process finished, the autoclave was let to cool down gradually to room temperature (RT) in the oven. The acid precipitation process is similar to the hydrothermal process, but the autoclave was kept at room temperature for 48 hours (technically we could count this method as a hydrothermal method at RT). The products of hydrothermal process or acid precipitation – aggregated slurry which was a suspension at the bottom of Teflon-shell -

was cleaned and filtrated three times with bi-distilled water and filter paper. The obtained products were then dried in ambient at 80 ^oC during 2 hours. The dried product was ground by agate mortar and pestled to get WO_3 powder.

2.2. Analytical methods

The pH of solution was measured by Hanna instruments (model HI2020-02) with the pH range from -2.000 to 16.000, and working temperature from -20 ^oC to 120 ^oC. The Field-Emission Scanning Electron Microscopy (FESEM) HITACHI S4800 was used to investigate the morphology of obtained samples. The crystalline properties of samples were obtained by using X'pert Pro (PANalytical) MPD with a CuKα radiation (λ = 1.54065 Å) at a scanning rate of $0.03^o/2s$ in the 2θ range from 10^0 to 70^0. The micro Raman spectroscopy was observed by Renishaw Invia Raman Microscope using 633-nm laser and Leica N PLAN L50x/0.50 BD Microscope objective.

3. RESULTS AND DISCUSSION

3.1. The morphology of samples

Figure 1 shows the FESEM images of four samples. In all four cases, WO_3 nanostructures with different morphologies were observed. Sample o-WO_3 had big nanoplate morphology (Figure 1a) with smooth surfaces and corners. Nanoplates are uniform with the various distribution of size. In similar conditions but temperature increased to 180^oC (sample m-WO_3) WO_3 nanoparticles are observed (Figure 1b). These nanoparticles have the smooth surface with sharp corners. The size of NPs diverse from 50x50 nm to 150x150 nm, but they all have a rectangular shape with the biggest dimension was about 150 nm.

When pH increased to 1.1, at 180^oC (sample h-WO_3) the mixture of nanorod with bundle of very small nanoparticles were observed (Figure 1c). The dimension of nanoparticles is about 40 nm which is in the same size with the diameter of nanorod. At 120^oC, with pH=1.7, these nanoparticles disappeared and only bundles of nanorods were observed (Figure 1.d). The diameter of nanorod is also approximate to the dimension of nanoparticle acquired at pH = 1.1. From FESEM images, it is clear that pH of precursor solution strongly affects the morphology of WO_3 nanostructures. The high acid concentration environment drives WO_3 molecules to make big structures. When pH value increased, WO_3 nanostructures tended to form structures with smaller dimension. But there is a critical value of pH, at which WO_3 nanostructures - nanoparticles get its minimum dimension. Above this value, nanoparticles tend to aggregate into nanorods (pH = 1.1 to 1.7). When acid environment got dilute, there was no aggregation obtained after the hydrothermal process (pH>2.5).

3.2. The XRD pattern of samples

To characterize the effect of synthesis parameters on crystallization of samples, XRD patterns of four samples were measured. Figure 2 exhibits the XRD patterns of four samples. All peaks in XRD pattern of o-WO_3 (Figure 2.a) are identified to orthorhombic structure $WO_3.H_2O$ (noted by star sign *) with space group Pmnb and lattice constant a = 0.5249 nm, b = 1.711 nm, c = 0.5133 nm, $\alpha = \beta = \gamma = 90^o$ (ICDD: 01-084-0886). But XRD analyses show that o-WO_3 was composed of two phases having the same orthorhombic structure, tungsten oxide hydrate $WO_3.H_2O$ and tungsten oxide $WO_{2.625}$ (ICDD: 01-081-1172). This result is reinforced by

scattering Raman spectra. The content of $WO_3.H_2O$ and $WO_{2.625}$ in o-WO_3 sample are 82% and 18%, respectively.

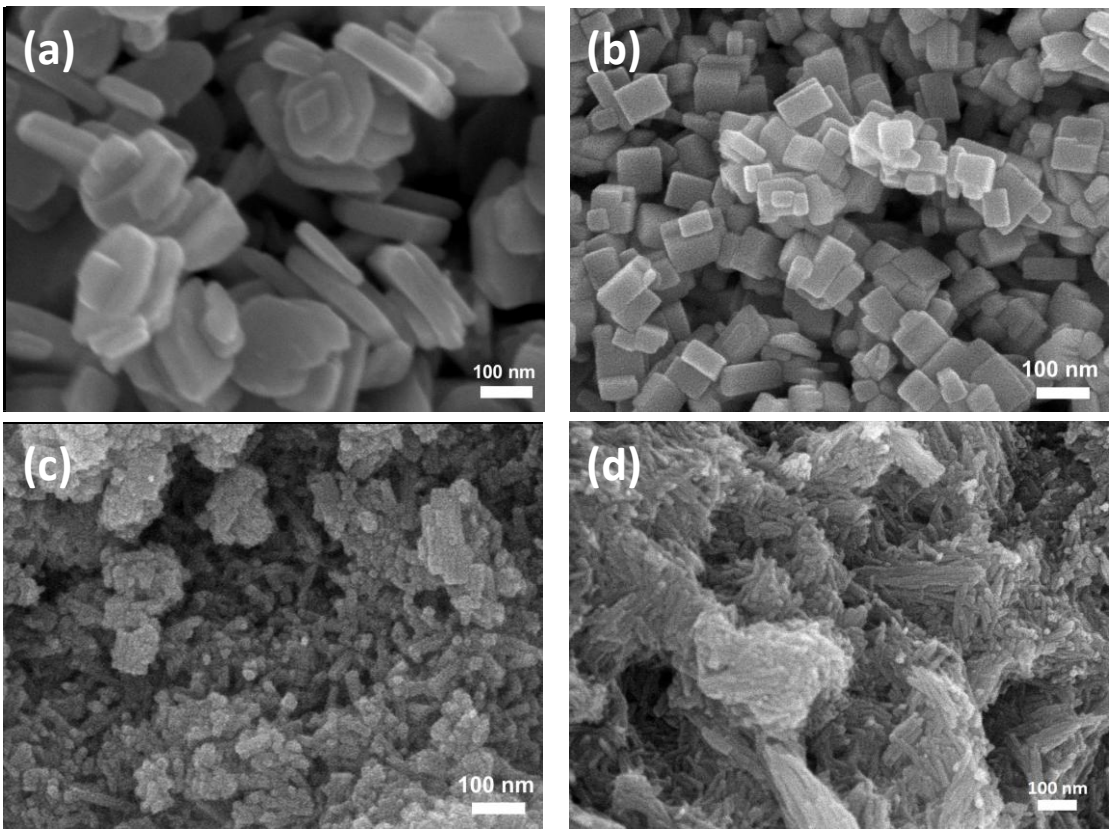

Figure 1. FESEM images of samples (a) large nanoplate o-WO_3, (b) nanoparticle m-WO_3, (c) mixture of nanorod with very small nanoparticle h-WO_3, and (d) the bundle of nanorod hn-WO_3.

In the XRD pattern of sample m-WO_3 (Figure 2.b), the peaks of two phases with the same monoclinic structure were recognized: WO_3 (60 % of content – marked with closed circles) and $W_{17}O_{47}$ (40 % of content and marked with hash sign #). Monoclinic WO_3 has space group P21/n and lattice constants a = 0.73013 nm, b = 0.75389 nm, c = 7.6893 nm, $\alpha = \gamma = 90^o$ and $\beta = 90.893^o$ (ICDD: 01-083-0951). $W_{17}O_{47}$ has monoclinic structure with P2/m space group and lattice structure a = 1.884 nm, b = 0.3787 nm, c = 1.233 nm, $\alpha = \gamma = 90^o$ and $\beta = 102.67^o$ (ICDD: 01-079-0171). Up to our knowledge, this is the first-time as-grown monoclinic nanostructure was observed. In other works, to get monoclinic structure, as-grown hexagonal WO_3 nanostructures were annealed up to 500^{o}C [8,9,16] but here monoclinic nanostructures could be obtained directly by hydrothermal method.

Figure 2.c shows the XRD pattern of h-WO_3 sample. In this pattern, all peaks were indexed to hexagonal structure tungsten oxide WO_3 (closed gray rectangular) with lattice constant a = 0.7298 nm; b = 0.7298 nm; c = 0.3899 nm, $\alpha = \beta = 90^o$, $\gamma = 120^o$ (ICDD: 01-075-2187). No evidence of other phase or impurities was obtained in analyzing XRD pattern. It means that the nanoparticles and nanorods have the same crystal structure. Moreover, nanoparticles had the same dimension as the diameter of nanorod (Figure 1.c). These results imply that nanoparticles are seeds of nanorods. To explain this phenomenon, we use the widely accepted theory which states that at the beginning of the hydrothermal process, nanoparticles were created, then

nanoparticles assembled in preference direction to form nanorod [7,17]. The strong acidic environment (pH < 1.0) prevented this assembly, when pH got to the higher value 1.67 – 1.8, nanoparticles mostly aggregated into nanorod and we obtained only bundle of nanorods as observed in Figure 1.d. The similarity between the XRD pattern of hn-WO_3 (Figure 2.d) and that of h-WO_3 (Figure 2.c) also supports this theory. Compared to the hn-WO_3 pattern, the XRD pattern of h-WO_3 is sharper, it implies that h-WO_3 has higher crystallization. This result is also supported by Raman spectra.

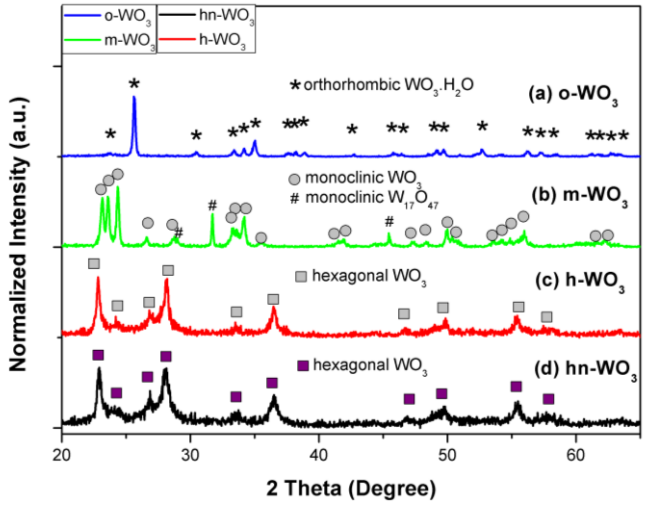

Figure 2. Normalized XRD patterns of samples (a) o-WO_3, (b) m-WO_3, (c) h-WO_3, and (d) hn-WO_3.

These XRD results exhibit the possibility to manipulate the crystalline structure of WO_3 from orthorhombic, to monoclinic and hexagonal by hydrothermal method and acid precipitation method. By changing the pH value from -1.0 to 1.1, the crystal structure of WO_3 nanostructures transforms from monoclinic to hexagonal. With pH = -1.0, by changing the temperature from RT to 180 ^oC, the morphology changes from nanoplate to nanoparticle in company with transformation of structure from metastable orthorhombic to the stable monoclinic pattern. It means that pH and temperature of hydrothermal process strongly affect the crystallization of WO_3 structures. Table 1 shows the evolution of morphology and structure of WO_3 nanostructures with the pH value and temperature.

Table 1. The structure, morphology and chemical formula of samples synthesized by hydrothermal method and acid precipitation (hydrothermal process at RT) with corresponding pH values and temperatures.

Name	pH*	Temperature	Morphology	Chemical formula	Structure
o-WO_3	-1.0	Room temperature	Nanoplate	$WO_3.H_2O$ and $WO_{2.625}$	Orthorhombic
m-WO_3	-1.0	180 ^oC	Nanoparticle	WO_3 and $W_{17}O_{47}$	Monoclinic
h-WO_3	1.1	180 ^oC	Nanorod and Nanoparticle	WO_3	Hexagonal
hn-WO_3	1.7	120 ^oC	Nanorod	WO_3	Hexagonal

(*: The value measured by Hanna HI2020-02 instrument.)

3.3. Raman spectroscopy of samples

In Figure 3, the normalized micro Raman spectra of samples are presented. In Raman spectra of o-WO_3 (Figure 3.a), there is a sharp and strong peak at wavenumber 945 cm^{-1} - corresponding to W^{6+} = O bond, which relates to the appearance of water molecular between layers of WO_6 octahedron [1, 18]. The water molecular causes the distortion of WO_6 octahedron and then causes an appearance of broadening the peak at 636 cm^{-1} which is assigned to be the stretching vibration of W^{6+}-O bond. Two peaks at 636 cm^{-1} and 945 cm^{-1} identify the appearance of water molecular in WO_3 structure [1, 18]. The weak peak at wavenumber 812 cm^{-1} is specified for the stretching mode of O-W^{6+}-O bond which supports the result of XRD analysis about the appearance of $WO_{2.625}$ phase in o-WO_3 sample.

The Raman spectrum of sample m-WO_3 (Figure 3.b) is the typical Raman spectrum of monoclinic WO_3 [18-21]. Two strong and sharp peaks at wavenumbers of 806 cm^{-1} and 717 cm^{-1} correspond to the stretching vibration of O-W^{6+}-O in octahedral WO_6. Three weaker peaks at 326 cm^{-1}, 273 cm^{-1}, and 241 cm^{-1} are assigned to the bending vibration of W^{6+}-O-W^{6+} bond of corner oxygen. The peaks at lower region (180 and 132 cm^{-1}) are attributed to the lattice vibration [18-21]. The presence of $W_{17}O_{47}$ phase is confirmed by the appearance of peak at 935 cm^{-1} corresponding to the lacking of oxygen in WO_6 octahedron.

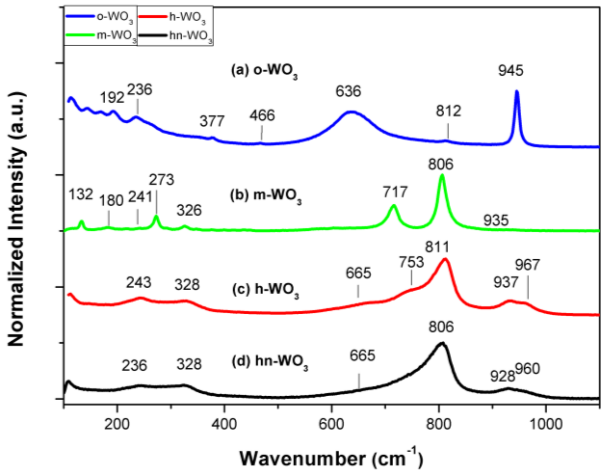

Figure 3. Normalized micro Raman spectra of WO_3 nanostructures: (a) o-WO_3, (b) m-WO_3, (c) h-WO_3, and (d) hn-WO_3.

Figure 3.c and 3.d show the Raman spectra of samples h-WO_3 and hn-WO_3, respectively. These patterns of spectra are similar, the reason is the sameness of crystal structure – hexagonal. The regions below 400 cm^{-1} wavenumber of two samples are alike corresponding to the same deformation and lattice vibration in the same crystal structure. The wide range spectra from 600 to 1000 cm^{-1} stands for the stretching mode of a typical hexagonal structure. The difference between two spectra is clearly shown in this region. In spectrum of h-WO_3, the peaks at 665, 753, 960 cm^{-1} are clearly showed but in hn-WO_3 these peaks almost disappear and become the shoulders of peaks at 806 and 928 cm^{-1}. The clearer peaks responses to the higher crystallization of sample h-WO_3 in higher acid concentration compare to sample hn-WO_3 synthesized in lower acid concentration. These results strengthen the role of pH on crystallization process of WO_3 nanostructures.

4. CONCLUSIONS

We have successfully synthesized WO_3 nanostructures with three different morphologies: nanoplate, nanoparticle and nanorod by hydrothermal and acid precipitation methods without using any structure-directing agent. The crystal of WO_3 nanostructures transformed from orthorhombic, monoclinic to hexagonal corresponding with the change of morphologies from nanoplate, nanoparticle to nanorod. With pH = -1.0, at room temperature, WO_3 had plate-like morphology with orthorhombic structure. Using the same condition, but higher temperature, WO_3 nanostructure obtained is nanoparticle type and has monoclinic crystal with less hydration. With pH = 1.1 at 180 ^oC, the nanorod appeared with bundle of very small nanoparticles which all had hexagonal structure. When pH gets to 1.7, only bundle of hexagonal nanorods was observed. These results imply a promising process to tailor the morphology and structure of WO_3 nanostructures without using any supporting agent, they also mean that it is possible to manipulate the optical, photocatalytic, electrochromic properties and surface state of WO_3 nanostructures for different applications. Up to our knowledge, this the first time monoclinic WO_3 nanoparticles were directly synthesized by hydrothermal method without using any supporting reactant. The mechanism of transforming from orthorhombic to monoclinic pattern in company with the dehydration process in WO_3 nanostructures at low pH value (pH = -1.0) is still unclear and needs more research.

Acknowledgments. This research was supported by Hanoi University of Science and Technology (HUST) under project number T2017-PC-134.

REFERENCES

1. Majid A., Maxime J. F. G. - Synthesis and characterization of tungstite ($WO_3.H_2O$) nanoleaves and nanoribbons, Acta Materialia **69** (2014) 203-209.
2. Imre M. S., Balázs F., Olivier R., Ágnes S., Péter N., Péter K., Gábor T., Balázs V., Katalin V. J., Krisztina L., Attila L. T., Péter B., Markku L. - WO_3 photocatalysts: Influence of structure and composition, Journal of Catalysis **294** (2012) 119-127.
3. Poongodi S., Suresh K. P., Masuda Y., Mangalaraj D., Ponpandian N., Viswanathan C., Ramakrishna S. - Synthesis of Hierarchical WO_3 nanostructured thin films with enhanced electrochromic performance for switchable smart windows, RSC Adv. **5** (2015) 96416-96427.
4. Kai H., Qingtao P., Feng Y., Shibing N., Xiucheng W., Deyan H. - Controllable synthesis of hexagonal WO_3 nanostructures and their application in lithium batteries, J. Phys. D: Appl. Phys. **41** (2008) 155417 (6pp).
5. Zhiwei L., Ping L., Yuan D., Qi W., Fuqiang Z., Alex A. Volinsky, Xuanhui Q. - Facile preparation of hexagonal $WO_3.0.33H_2O$/C nanostructures and its electrochemical properties for lithium-ion batteries, Applied Surface Science **394** (2017) 70–77.
6. Ying Peng X., Gang L., Lichang Y., Hui-Ming C. - Crystal facet-dependent photocatalytic oxidation and reduction reactivity of monoclinic WO_3 for solar energy conversion, J. Mater. Chem. **22** (2012) 6746
7. Tianyou P., Dingning K., Jiangrong X., Li W., Jun H., Ling Z. - Hexagonal phase WO_3 nanorods: hydrothermal preparation, formation mechanism and its photocatlytic O_2

produciton under visible-light irradiation, Journal of Solid state chemistry **194** (2012) 250-256.

8. Dien N. D., Vuong D. D., Chien N. D. - Hydrothermal synthesis and NH_3 gas sensing property of WO_3 nanorods at low temperature, Adv. Nat. Sci.: Nanosci. Nanotechnol. **6** (2015) 035006-035012.
9. Tong P. V., Hoa N. D., Quang V. V., Duy N. V., Hieu N. V. - Diameter controlled synthesis of tungsten oxide nanorod bundles for highly sensitive NO2 gas sensors, Sensors and Actuators B **183** (2013) 372– 380.
10. Filipescu M., Ion V., Colceag D., Ossi P. M., Dinescu M.- Growth and characterizations of nanostructured tungsten oxides, Thin Solid Films **408** (2002) 302-309.
11. Marques A. C., Santos L., Costa M. N., Dantas J. M., Duarte P., Gonçalves A., Martins R., Salgueiro C. A., Fortunato E. - Office paper platform for bioelectrochromic detection of electrochemically active bacteria using tungsten trioxide nanoprobes, Scientific Reports **5** (2015) 9910.
12. Rajagopal S., Nataraj D., Mangalaraj D., Djaoued Y., Robichaud J., Khyzhun O. Y. - Controlled growth of WO3 nanostructures with three different morphologies and their structural, optical, and photodecomposition studies, Nanoscale Res Lett **4** (2009) 1335–1342.
13. Kenneth P. R., Ramanan A., Whittingham M. S. - Hydrothermal synthesis of sodium tungstates, Chem. Mater. **2** (1990) 219-221.
14. Pu L., Xing L., Ziyan Z., Mingshan W., Thomas F., Qian Z., Ying Z.- Correlations among structure, composition and electrochemical performances of WO3 anode materials for lithium ion batteries, Electrochimica Acta **192** (2016) 148–157.
15. Zheng J. Y., Haider Z., Van K. T., Pawar A. U., Kang M. J., Kim C. W., Kang Y. S. - Tuning of the crystal engineering and photoelectrochemical properties of crystalline tungsten oxide for optoelectronic device applications, CrystEngComm, **17** (2015) 6070-6093.
16. Kalanur S. S., Hwang Y. J., Chae S. Y., Joo O. S. - Facile growth of aligned WO_3 nanorods on FTO substrate for enhanced photoanodic water oxidation activity, J. Mater. Chem. A **1** (2013) 3479.
17. Fenglin L., Xianjie C., Qinghua X., Lihong T., Xiaobo C. - Ultrathin tungsten oxide nanowires: oleylamine assisted nonhydrolytic growth, oxygen vacancies and good photocatalytic properties, RSC Adv. **5** (2015) 77423-77428.
18. Daniel M. F., Desbat B., Lassegues J. C., Gerand B., Figlarz M. - Infrared and Raman study of WO_3 tungsetn trioxides and WO_3,xH_2O tungsten trioxide hydrates, Journal of Solid state chemistry **67** (1987) 235-247.
19. Ramana C. V., Utsunomiya S., Ewing R. C., Julien C. M., Becker U. - Structural stability and phase transitions in WO_3 thin films, J. Phys. Chem. B **110** (2006) 10430-10435.
20. Jarupat S., Titipun T., Somchai T.- Photocatalysis of WO_3 Nanoplates synthesized by conventional hydrothermal and microwave-hidrothermal methods and of commercial WO_3 nanorods, Journal of Nanomaterials, **2014**, ID 739251.
21. Yesheng L., Zilong T., Junying Z., Zhongtai Z. - Enhanced photocatalytic performance of tungsten oxide through tuning exposed facets and introducing oxygen vacancies, Journal of Alloys and Compounds **708** (2017) 358-366.